PLANT SCIENCE

Organic acids and glucose prime late-stage fungal biotrophy in maize

Matthias Kretschmer[1], Djihane Damoo[1], Sherry Sun[1]†, Christopher W. J. Lee[1], Daniel Croll[2], Harry Brumer[3], James Kronstad[1]*

Many plant-associated fungi are obligate biotrophs that depend on living hosts to proliferate. However, little is known about the molecular basis of the biotrophic lifestyle, despite the impact of fungi on the environment and food security. In this work, we show that combinations of organic acids and glucose trigger phenotypes that are associated with the late stage of biotrophy for the maize pathogen *Ustilago maydis*. These phenotypes include the expression of a set of effectors normally observed only during biotrophic development, as well as the formation of melanin associated with sporulation in plant tumors. *U. maydis* and other hemibiotrophic fungi also respond to a combination of carbon sources with enhanced proliferation. Thus, the response to combinations of nutrients from the host may be a conserved feature of fungal biotrophy.

Fungi threaten human health, crop production, and food security (*1*, *2*). Many economically important fungal pathogens of plants are obligate biotrophs that cannot be propagated outside of the host (*3*). Obligate biotrophs also include beneficial mycorrhizal fungi that provide critical nutrients such as phosphate to 80% of plant species (*4*). In general, there is a lack of information about the nutritional requirements for fungal proliferation and development in host tissue, although genome analyses suggest that the loss of specific biosynthetic capabilities conditions a reliance on host nutrients (*3*, *5*).

The maize fungal pathogen *Ustilago maydis* can be grown axenically in culture but is obligately dependent on a plant host to complete the sexual phase of its life cycle (*6*–*8*). This phase involves the mating of compatible sporidia to establish invasive filaments; the delivery of effector proteins; the induction of conspicuous tumors on leaves, ears, and tassels; and the formation of massive numbers of melanized spores in tumors (*8*). In addition to the economic impact of *U. maydis* on maize production, the fungus is unusual because the tumor tissue has been prized as a culinary delicacy in Mexico since the time of the Aztecs (*9*).

Induction of biotrophic phenotypes in culture

During infection, *U. maydis* reprograms developing tumor tissue into a sink for photosynthate, and the carbon sources available to the fungus include carbohydrates and organic

[1]Michael Smith Laboratories and Department of Microbiology and Immunology, University of British Columbia, Vancouver, BC, Canada. [2]Laboratory of Evolutionary Genetics, Institute of Biology, Université de Neuchâtel, Neuchâtel, Switzerland. [3]Michael Smith Laboratories and Department of Chemistry, University of British Columbia, Vancouver, BC, Canada.
*Corresponding author. Email: kronstad@msl.ubc.ca
†Present address: Department of Botany, University of British Columbia, Vancouver, BC, Canada.

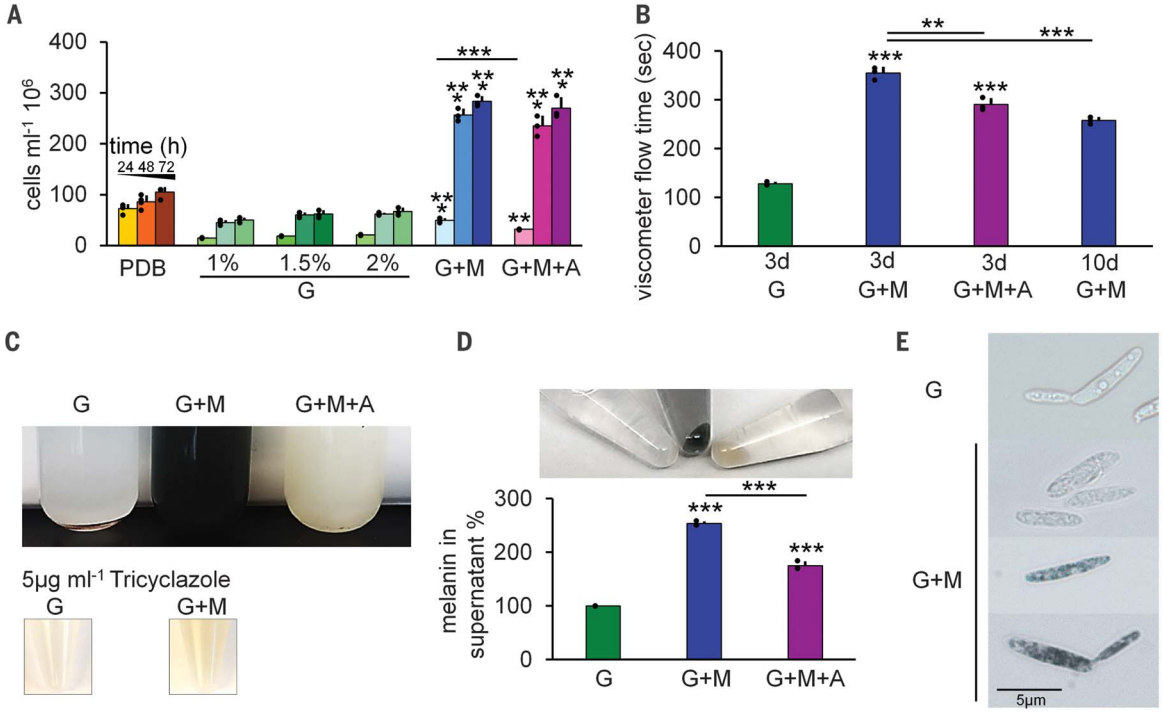

Fig. 1. Carbon sources influence proliferation, extracellular polysaccharide, and melanin. (**A**) Cell numbers were compared upon growth in minimal medium with different concentrations of glucose (G), glucose plus malate (G+M), glucose plus malate with aeration (G+M+A), or potato dextrose broth (PDB). The G+M and G+M+A conditions were compared with the G 1.5% condition. (**B**) Culture viscosity to detect extracellular polysaccharide was measured after 3 or 10 days of growth with a viscometer and is reported in seconds of flow time. (**C**) Detection of melanin in *U. maydis* cultures in G, G+M, or G+M+A after 72 hours of growth. Melanin formation in the G+M medium is inhibited with 5 µg ml^{-1} of tricyclazole. (**D**) Melanin is associated with cell pellets and is measurable in culture supernatants. (**E**) Melanin is cell associated with a range of intensities. In (A), (B), and (D), lines above the bar graphs indicate the statistical significance for the comparisons at the ends of each line. Significance levels for comparisons of the wild-type strain in different media are $^{**}P \leq 0.01$ and $^{***}P \leq 0.001$ according to analysis of variance (ANOVA) with a Tukey procedure as a post hoc test. Error bars indicate SD.

acids (*7*, *10*–*14*). Given that maize plants carry out C4 photosynthesis of the nicotinamide adenine dinucleotide phosphate (NADP)–malic enzyme subtype in which 75% of CO_2 is initially fixed into malate, we hypothesized that metabolic adaptation to organic acids is a key determinant of biotrophic proliferation for *U. maydis* (*7*, *15*). We tested this hypothesis by culturing the fungus in standard glucose medium with the addition of malate [glucose plus malate (G+M)] and found that this combination stimulated cell proliferation, increased culture viscosity, and triggered the accumulation of dark, pigmented cells (Fig. 1 and figs. S1 and S2). Other organic acids also triggered the same phenotypes in combination with glucose (fig. S3 and table S1). The increase in viscosity was due to the accumulation of extracellular polysaccharides with a β-1,3 glucan structure commonly found in fungi (fig. S2). The pigment was cell associated and was related to melanin, as determined with the specific inhibitor tricyclazole (Fig. 1, C to E, and fig. S1). These phenotypic changes prompted an investigation of the relevance of the observed responses to the biotrophic development of *U. maydis* in maize. We therefore examined melanin formation, the role of organic acid transporters, the transcription of genes for biotrophic effectors, and the contributions of mitochondrial functions and oxygen.

Melanin formation during *U. maydis* sporulation in tumors is catalyzed by the laccase Lac1 and the polyketide synthase Pks1 (*16*). However, additional enzymes may contribute to melanin formation because the genome encodes five other candidate laccases and four additional polyketide synthases (*17*, *18*). RNA sequencing analysis of cells grown in glucose (G) versus cells from the G+M condition revealed that the transcripts for three *pks* genes (*pks3*, *pks4*, and *pks5*) were elevated in the G+M condition (Fig. 2A, figs. S4 and S5, and tables S2 and S3). These *pks* genes are present in a cluster of 15 genes on chromosome 12, and their transcript levels are regulated by the transcription factor Mtf1 encoded within the cluster (Fig. 2A) (*18*). Ten genes in this cluster, including *mtf1* (up-regulated 1714-fold), are expressed at a late stage of infection [12 days post-inoculation (dpi)] (*14*). The transcripts for *mtf1* were elevated in the G+M condition, and we found that an *mtf1* deletion mutant did not

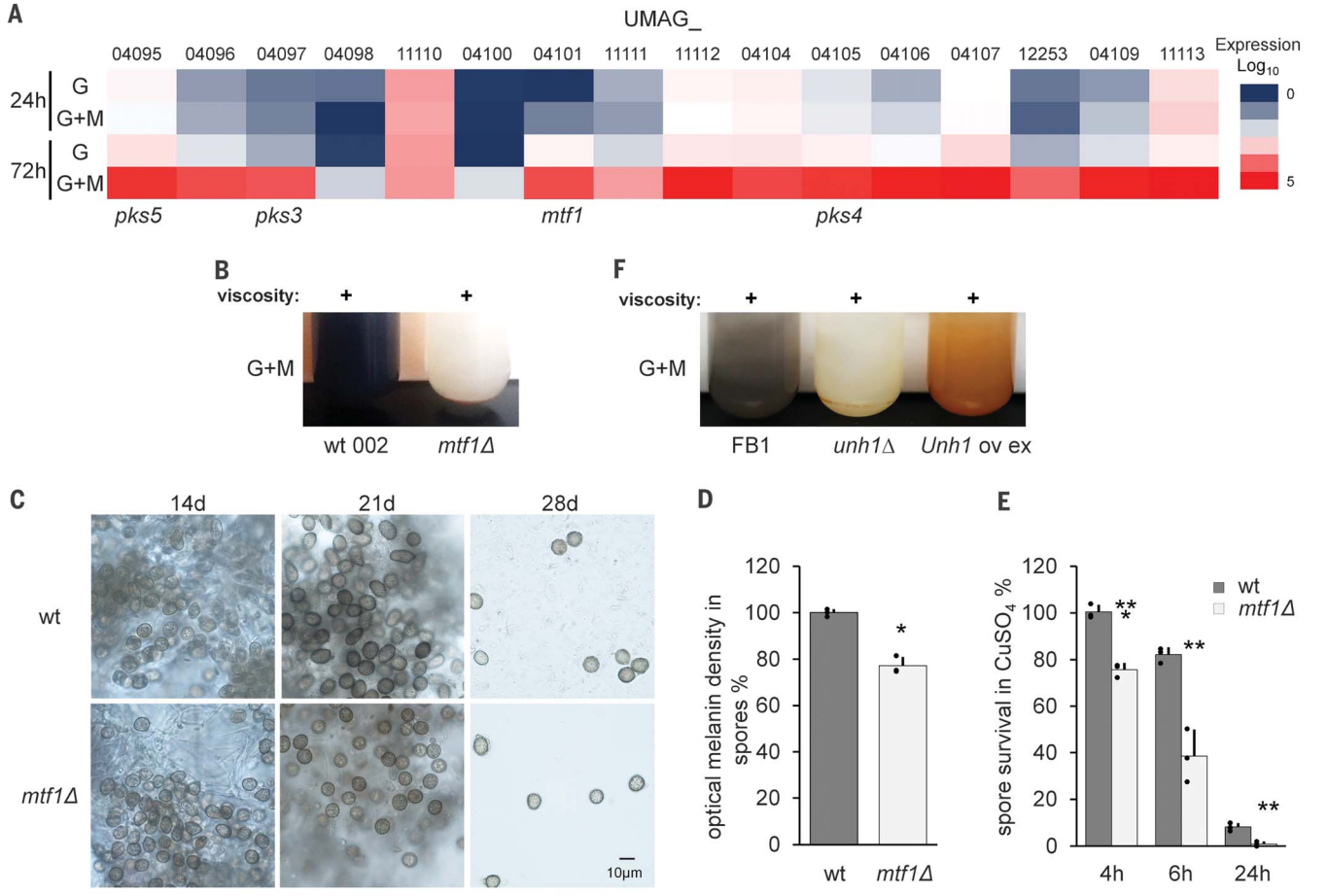

Fig. 2. Regulation and contributions of a melanin gene cluster. (**A**) A gene cluster encodes the transcriptional regulator Mtf1 and three polyketide synthases. The heatmap shows averaged normalized expression values of three biological replicates for G and G+M at 24 and 72 hours. The expression values were $\log_{10}$ transformed; the color code for the $\log_{10}$ scale is from 0 (low expression; dark blue) to 5 (high expression; red). Sample expression values between 0 and 1 were set to 1 before $\log_{10}$ transformation. (**B**) Melanin is reduced in the *mtf1*Δ mutant upon growth in G+M medium. wt, wild type. (**C**) Spores of the *mtf1*Δ mutant have reduced melanin formation over time during infection of maize seedlings. (**D**) Optical measurement of melanin revealed reduced content in spores of the *mtf1*Δ mutant at 28 days. (**E**) Survival of *mtf1*Δ spores is reduced upon treatment with $CuSO_4$. (**F**) Deletion or overexpression of the sporulation transcription factor *unh1* influences melanin formation. In (D) and (E), significance levels for comparisons of mutant and wild-type strains are $^*P \le 0.05$, $^{**}P \le 0.01$, and $^{***}P \le 0.001$ according to *t* test or ANOVA with a Tukey procedure as a post hoc test. Error bars indicate SD.

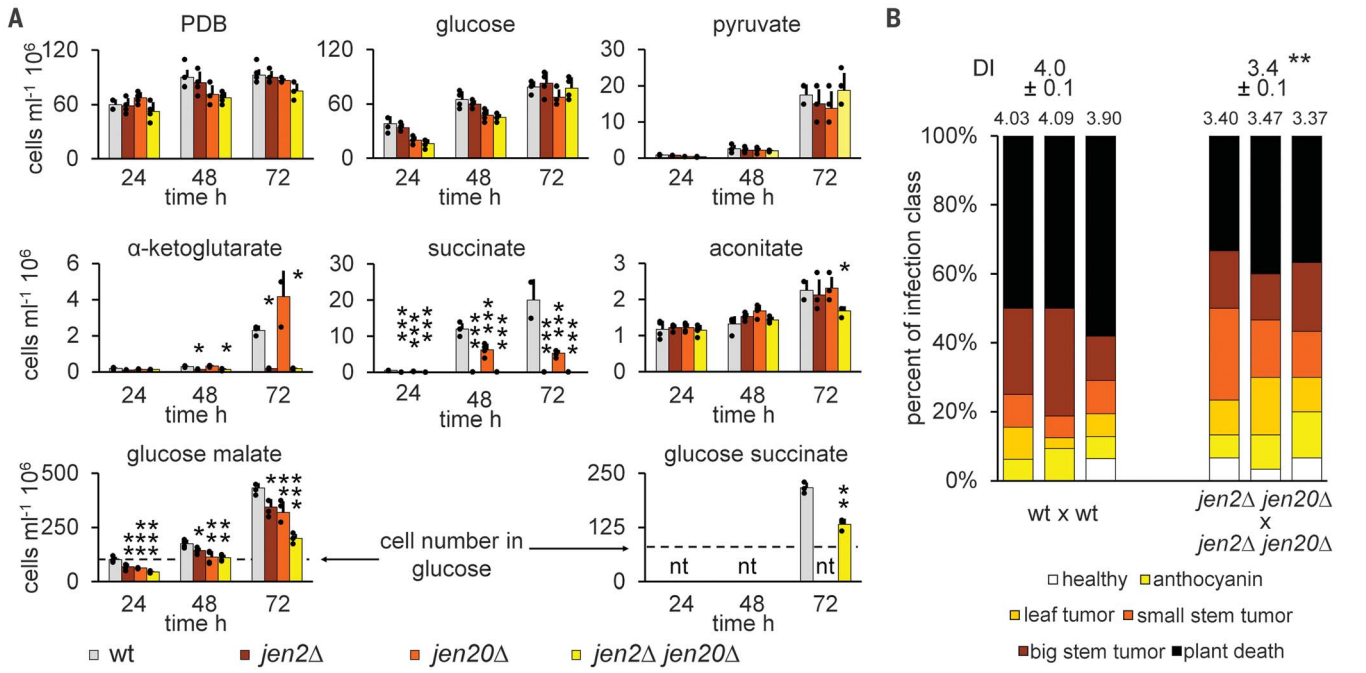

Fig. 3. Candidate transporters influence growth on dicarboxylates and virulence. (**A**) The *jen2*Δ and *jen20*Δ mutants have impaired growth on carboxylates and a combination of glucose and dicarboxylates. (**B**) Virulence of the *jen2*Δ *jen20*Δ double mutant is reduced on maize seedlings. Significance levels for comparisons of mutant and wild-type strains are $*P \leq 0.05$, $**P \leq 0.01$, and $***P \leq 0.001$ according to a *t* test for infection or ANOVA with a Tukey procedure as a post hoc test. A Kruskal-Wallis with Dunn analysis as a post hoc test was used to evaluate growth on aconitate. Error bars indicate SD. DI, disease index; nt, not tested.

form melanin during growth in G+M medium. Furthermore, the mutant showed reduced melanin content in spores from tumor tissue (Fig. 2, C and D). That is, the mutant caused disease in maize seedlings, which led to spore development, but the melanin content of isolated *mtf1*Δ spores was reduced by 22.8% (Fig. 2D). Additionally, the *mtf1*Δ spores showed incomplete maturation because their survival was reduced upon $CuSO_4$ treatment compared with wild-type spores (Fig. 2E).

The transcription factor Unh1 also regulates sporulation in *U. maydis*, and *unh1* transcripts were elevated during growth on G and G+M media at 72 hours versus G at 24 hours, as well as in infected plants (table S3) (*17*, *19*). The *unh1*Δ mutant was also compromised for melanin formation on G+M, thus further linking in planta sporulation to the melanin phenotype induced in culture (Fig. 2F). Complementation of the *unh1*Δ mutation resulted in a modified pigment color, perhaps due to overexpression of the gene (Fig. 2F) (*19*). In addition to Unh1, several other virulence-associated regulatory factors, including protein kinases and transcription factors, also influenced melanin formation in the G+M condition (fig. S6). Therefore, these functions are candidate components of a regulatory network for melanin formation. Overall, these results suggest that *U. maydis* has one melanin biosynthesis pathway that is dependent on Lac1 and Pks1 and a second pathway that is regulated by Mtf1 and Unh1; the latter pathway is induced during sporulation in planta and in response to growth in glucose plus organic acids.

The relevance of the response to organic acids for biotrophy was tested further by constructing mutants that lacked dicarboxylate transporters and examining virulence in maize seedlings. We mined the genome to identify candidate transporters and examined their transcript levels in cells from the G+M condition (tables S2, S4, and S5). From this analysis, we identified two dicarboxylate transporters, Jen2 and Jen20, that were required for robust growth on specific organic acids (e.g., aconitate, α-ketoglutarate, succinate, or malate) and in combination with glucose (Fig. 3A). Deletion of both *jen2* and *jen20* attenuated virulence on maize, although some disease symptoms still occurred, indicating that additional transporters contribute to in planta growth (Fig. 3B). Overall, these results indicate that the ability to acquire organic acids contributes to the virulence of *U. maydis* on maize.

In vitro expression of disease effectors

The delivery of effector proteins to suppress plant defense and promote virulence is a key aspect of biotrophic development (*14*). For *U. maydis*, candidate effectors are expressed in transcriptional modules of coexpressed genes at defined stages of infection, including plant surface interactions, establishment of biotrophy, nutrient acquisition, and induction of tumors (*14*, *20*). Many of the effectors are expressed only during growth in the host and define virulence-specific modules (*14*). We compared the transcriptional response to the G and G+M conditions with the established modules and found that transcripts encoding a subset of effectors involved in biotrophic development were elevated in response to carbon sources (figs. S7 to S9 and table S2). That is, the transcript levels for some effectors were more highly elevated in G+M at 72 hours than in either G at 24 hours or G at 72 hours, as was demonstrated for the specific effectors Eff1-1, Ten1, Rsp3, Afu1-3, Mig2-2, and Rrm67 (fig. S8) (*20*). Some of the effector genes also displayed elevated transcripts in G at 72 hours versus G at 24 hours, indicating a response to glucose depletion during the stationary phase. These effectors included the Afu3, See1, Pit2, Cmu1, Stp1, Stp4, Mig2-4, and Eff1 proteins (fig. S8 and table S2) (*20*, *21*). Many of the effector genes in *U. maydis* are found in clusters that affect virulence upon deletion (fig. S9) (*7*). In this regard, transcripts for genes in the major virulence clusters 2A, 6A, 10A, and 19A were elevated in the G+M at 72 hours condition

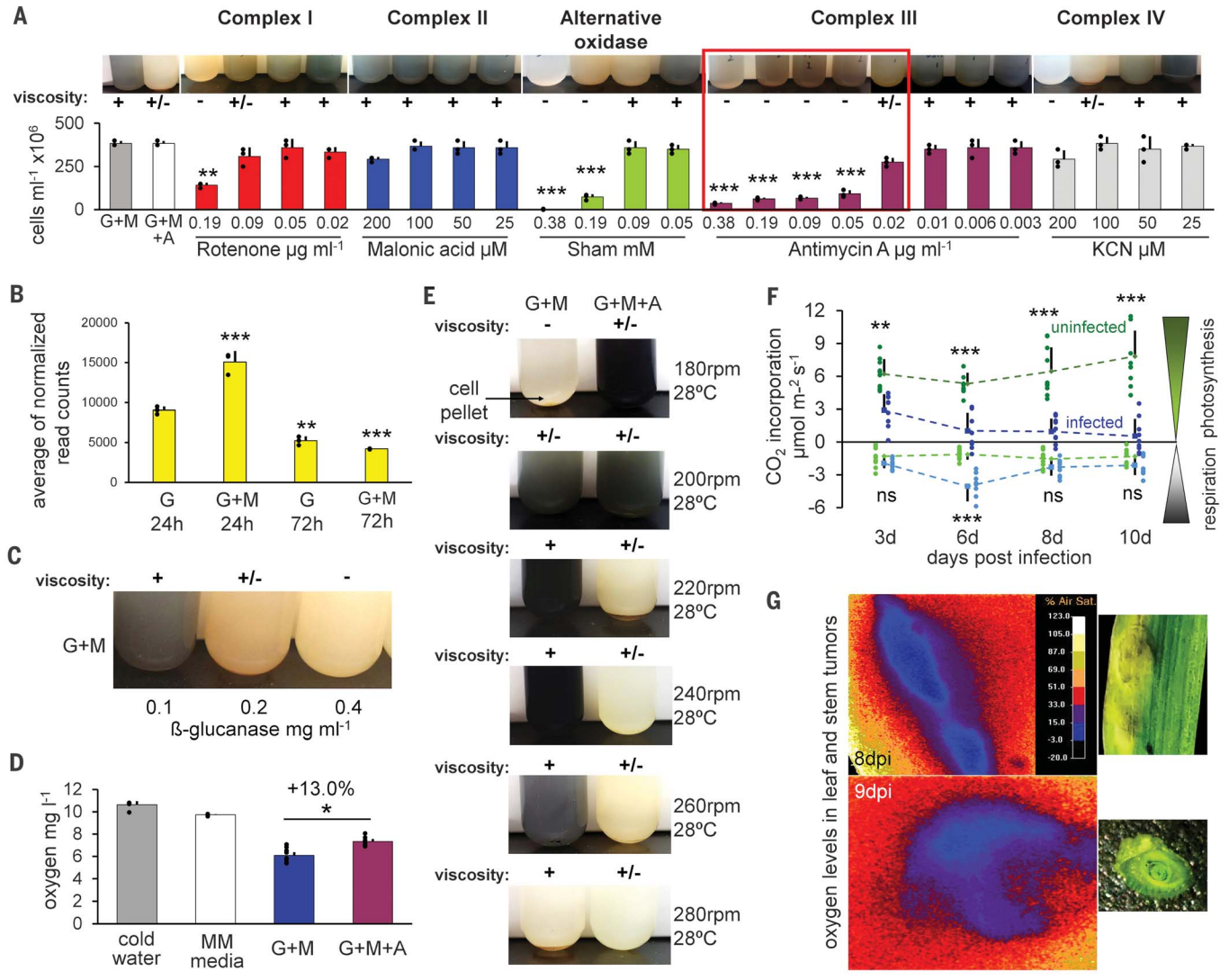

Fig. 4. Mitochondrial functions and oxygen contribute to biotrophic phenotypes. (**A**) Inhibition of electron transport chain complexes influences growth, culture viscosity, and melanin status in G+M. The red frame indicates melanin formation in cultures with growth inhibition. (**B**) Analysis of the normalized transcript levels of 155 genes with elevated transcript levels in the yellow general growth module (*14*) in G+M at 24 hours. Of these genes, 49 encode mitochondrial proteins. The expression of Fe-S cluster and electron transport chain genes can be found fig. S11 and table S2. (**C**) Influence of β-glucanase treatment on viscosity and melanin formation. (**D**) Oxygen levels in G+M cultures at 72 hours were measured and compared with those in cold water, uninoculated minimal medium (MM), and G+M+A cultures. (**E**) Melanin formation and culture viscosity are dependent on aeration as influenced by shaker speed. (**F**) Photosynthesis and respiration rates of control maize leaves (green) and infected leaves (blue) during a time course of infection. The dashed lines indicate trends over time. ns, not significant. (**G**) Two-dimensional depiction of oxygen levels in planta during infection at 8 and 9 dpi in leaves and stems with tumors. Yellow and orange, high oxygen levels; blue, low oxygen levels. Significance levels for comparisons between treated and untreated cells (A), between G and G+M (B), and between infected and uninfected tissue at each time point (F) are $*P \leq 0.05$, $**P \leq 0.01$, and $***P \leq 0.001$ according to a *t* test for oxygen measurement or ANOVA with a Tukey procedure as a post hoc test. Error bars indicate SD.

versus in G at 72 hours (fig. S9 and table S2). Transcript levels for genes in other clusters were also elevated in the G+M conditions (fig. S10). These clusters contained genes for the biosynthesis of itaconic acid and the siderophore ferrichrome A that are highly expressed in vivo (*22*), as well as genes for melanin and primary or secondary metabolism (fig. S10 and table S3). Overall, we conclude that the G+M culture condition triggers the transcription of genes normally expressed only during biotrophic growth in planta.

Mitochondrial functions and oxygen influence biotrophy

Mitochondrial functions and oxygen sensing play roles in the metabolic adaptation of fungi to the host environment (*23*). We found that mitochondrial functions (e.g., electron transport chain components and Fe-S–requiring proteins) were enriched in the Functional Catalogue (FunCat) analysis of the transcriptome data (figs. S4 and S11 and tables S2 and S6). We identified 155 genes in the module of general growth (*14*) that had elevated transcripts at 24 hours in G+M versus G; one-third of these genes are annotated as encoding mitochondrial

proteins. Transcripts related to Fe-S cluster–containing proteins of the electron transport chain complexes I to III, as well as transcripts for other components of complexes I to III and alternative oxidase, were elevated in the G+M condition (Fig. 4, A and B, and tables S2 and S6). We therefore tested the influence of inhibition of electron transport chain complexes on the response to mixed carbon sources and found that inhibitors of complex I, the alternative oxidase, and complex IV reduced melanin and culture viscosity but allowed growth in the G+M condition (Fig. 4A). In particular, inhibition of complex III reduced growth and viscosity, but melanin formation was still observed, perhaps indicating an uncoupling of pigmentation and proliferation.

Oxygen is the terminal electron acceptor in the electron transport chain, so we examined conditions with enhanced aeration (A) to assess the role of oxygen in melanin formation (G+M+A) (Fig. 4, C to E). Specifically, aeration was enhanced in the G+M condition by the addition of β-glucanase to reduce viscosity, which led to a concentration-dependent reduction in melanin (Fig. 4C). The G+M+A cultures resulted in 13% higher oxygen levels than the G+M condition (Fig. 4D), and the speed of culture shaking influenced melanin formation, as expected for a negative influence of oxygen (Fig. 4E and fig. S1). It is possible that oxygen could affect not only mitochondrial functions but also oxidation reactions that influence the polymerization of melanin precursors. Oxygen levels may also be relevant during pathogenic development in planta, especially given that infection negatively influences transcript levels for chloroplast genes, including those encoding photosynthetic functions (*24*, *25*). We evaluated the rates of photosynthesis and respiration and found that photosynthesis was inhibited in infected tissue, especially during tumor formation, whereas respiration peaked at 6 dpi (Fig. 4F). The observed down-regulation of photosynthesis is consistent with the results of previous studies (*25*). Noninvasive two-dimensional oxygen measurements confirmed that oxygen levels were also reduced in tumor tissue (Fig. 4G). We conclude that reduced oxygen tension is required for the in vitro biotrophic response to organic acids. Along with the impact of electron transport chain inhibition, this result implicates the mitochondria and mitochondrial functions as potential regulators of fungal biotrophy, perhaps through an influence on metabolite concentrations and the generation of signals that regulate gene expression.

We also tested additional fungal species for enhanced proliferation, viscosity, or pigmentation in media with glucose and organic acids to determine whether the response might be a general feature of biotrophic and hemibiotrophic fungi (fig. S12). We did not see an influence on the human pathogens *Candida albicans* and *Cryptococcus neoformans*, the saprophyte *Saccharomyces cerevisiae*, the mycorrhizal fungus *Laccaria bicolor*, or the necrotrophic plant pathogen *Sclerotinia sclerotiorum*. By contrast, the biotrophic and hemibiotrophic fungi *Ustilago hordei*, *Sporisorium reilianum*, *Fusarium oxysporum*, and *Verticillium dahliae* showed increased cell numbers or growth rates on the G+M medium compared with on G alone (fig. S12). Therefore, the response to mixed carbon sources may be a conserved feature of some biotrophic and hemibiotrophic fungi.

This study reveals a complex response of *U. maydis* to organic acids that involves mitochondrial functions, oxygen sensing, specific transporters, and transcriptional regulators of traits related to biotrophy. We also observed an accumulation of β-glucan in our culture conditions. This extracellular polysaccharide is a likely component of the mucilage matrix that accumulates during sporulation in tumors (*26*). The response to combinations of carbon sources may be a conserved feature of biotrophic fungal pathogens as well as other microbes that associate with plants. For example, obligate mycorrhizal fungi respond to lipids and sugars with proliferation and pre-spore formation, and rhizobia bacteria respond to dicarboxylates such as succinate and malate from legume hosts during nodulation and nitrogen fixation (*27*–*31*). Furthermore, features of bacterial nodulation such as extracellular polysaccharide production, malate metabolism, and oxygen sensing are shared with fungal tumor formation (*32*, *33*). The response to defined combinations of nutrients may therefore be a general theme in plant-microbe interactions.

REFERENCES AND NOTES

1. M. C. Fisher *et al*., *mBio* **11**, e00449-20 (2020).
2. J. B. Ristaino *et al*., *Proc. Natl. Acad. Sci. U.S.A.* **118**, e2022239118 (2021).
3. P. D. Spanu, R. Panstruga, *Front. Plant Sci.* **8**, 192 (2017).
4. N. Ferrol, C. Azcón-Aguilar, J. Pérez-Tienda, *Plant Sci.* **280**, 441–447 (2019).
5. P. D. Spanu *et al*., *Science* **330**, 1543–1546 (2010).
6. J. J. Christensen, "Corn smut caused by *Ustilago maydis*" (American Phytopathology Society Monograph no. 2, American Phytopathology Society, 1963).
7. J. Kämper *et al*., *Nature* **444**, 97–101 (2006).
8. W. Zuo *et al*., *Annu. Rev. Phytopathol.* **57**, 411–430 (2019).
9. M. Juárez-Montiel, S. Ruiloba de León, G. Chávez-Camarillo, C. Hernández-Rodríguez, L. Villa-Tanaca, *Rev. Iberoam. Micol.* **28**, 69–73 (2011).
10. R. J. Horst, T. Engelsdorf, U. Sonnewald, L. M. Voll, *J. Plant Physiol.* **165**, 19–28 (2008).
11. R. J. Horst *et al*., *Plant Physiol.* **152**, 293–308 (2010).
12. D. Sosso *et al*., *Plant Physiol.* **179**, 1373–1385 (2019).
13. M. Ludwig, *Front. Plant Sci.* **7**, 647 (2016).
14. D. Lanver *et al*., *Plant Cell* **30**, 300–323 (2018).
15. M. D. Hatch, *Biochem. J.* **125**, 425–432 (1971).
16. E. Islamovic *et al*., *Mol. Plant Microbe Interact.* **28**, 42–54 (2015).
17. M. Tollot *et al*., *PLOS Pathog.* **12**, e1005697 (2016).
18. E. Z. Reyes-Fernández, Y. M. Shi, P. Grün, H. B. Bode, M. Bölker, *Appl. Environ. Microbiol.* **87**, e01510-20 (2021).
19. C. E. Doyle, H. Y. Kitty Cheung, K. L. Spence, B. J. Saville, *Fungal Genet. Biol.* **94**, 54–68 (2016).
20. D. Lanver *et al*., *Nat. Rev. Microbiol.* **15**, 409–421 (2017).
21. M. Schuster, G. Schweizer, R. Kahmann, *Fungal Genet. Biol.* **112**, 21–30 (2018).
22. M. Kretschmer, D. Croll, J. W. Kronstad, *Mol. Plant Pathol.* **18**, 1222–1237 (2017).
23. B. Black, C. Lee, L. C. Horianopoulos, W. H. Jung, J. W. Kronstad, *PLOS Pathog.* **17**, e1009661 (2021).
24. M. Kretschmer, D. Croll, J. W. Kronstad, *Mol. Plant Pathol.* **18**, 1210–1221 (2017).
25. G. Doehlemann *et al*., *Plant J.* **56**, 181–195 (2008).
26. F. Banuett, I. Herskowitz, *Development* **122**, 2965–2976 (1996).
27. L. H. Luginbuehl *et al*., *Science* **356**, 1175–1178 (2017).
28. Y. Jiang *et al*., *Science* **356**, 1172–1175 (2017).
29. A. Keymer *et al*., *eLife* **6**, e29107 (2017).
30. Y. Sugiura *et al*., *Proc. Natl. Acad. Sci. U.S.A.* **117**, 25779–25788 (2020).
31. C. C. M. Schulte *et al*., *Sci. Adv.* **7**, eabh2433 (2021).
32. S. Acosta-Jurado, F. Fuentes-Romero, J. E. Ruiz-Sainz, M. Janczarek, J. M. Vinardell, *Int. J. Mol. Sci.* **22**, 6233 (2021).
33. A. L. Le Gac, T. Laux, *Mol. Plant* **12**, 1422–1424 (2019).

ACKNOWLEDGMENTS

We thank G. Bakkeren, F. Banuett, G. Braus, C. Haney, K. Heimel, R. Kahmann, M. Perlin, and B. Saville for fungal strains and K. Heimel for insightful comments. We also thank the Department of Civil Engineering at UBC for the use of the oxygen meter and the Department of Botany for the use of the photosynthesis meter. **Funding:** This work was supported by a grant from the Natural Sciences and Engineering Research Council of Canada and by an NSERC-CREATE program (to J.K.) and by the Chemical Sciences, Geosciences and Biosciences Division, Office of Basic Energy Sciences, US Department of Energy, grant (DE-SC0015662) to Parastoo Azadi at the Complex Carbohydrate Research Center. J.K. is a Burroughs Wellcome Fund Scholar in Molecular Pathogenic Mycology and a fellow of the CIFAR program: Fungal Kingdom Threats & Opportunities. **Author contributions:** Conceptualization: M.K. and J.K.; Methodology: M.K., D.D., S.S., and H.B.; Investigation: M.K., D.D., S.S., C.W.J.L., D.C., and H.B.; Visualization: M.K. and D.C.; Funding acquisition: J.K.; Project administration: J.K.; Supervision: J.K. and M.K.; Writing – original draft: M.K., J.K.; Writing – review and editing: M.K., J.K., D.D., S.S., C.W.J.L., D.C., and H.B. **Competing interests:** The authors declare that they have no competing interests. **Data and materials availability:** The RNA sequencing data for the comparisons of transcript levels for cells grown in G medium versus G+M (with and without additional aeration) are available at the Gene Expression Omnibus with the accession number GSE194157 for the project and accession numbers GSM5829810 to GSM5829827 for the samples. All other data needed to evaluate the conclusions in the paper are present in the paper or the supplementary materials, and all materials are available from the authors without restriction.

SUPPLEMENTARY MATERIALS

science.org/doi/10.1126/science.abo2401
Materials and Methods
Figs. S1 to S12
Tables S1 to S8
References (*34*–*63*)
MDAR Reproducibility Checklist

View/request a protocol for this paper from *Bio-protocol*.

Submitted 21 January 2022; accepted 4 May 2022
10.1126/science.abo2401